Performance Comparisons of Conventional and Line-Focused Surface Raman Spectrometers

JEREMY RAMSEY, SRIKANTH RANGANATHAN, RICHARD L. McCREERY,* and JUN ZHAO

Department of Chemistry, The Ohio State University, 100 W. 18th Ave. Columbus, Ohio (J.R., S.R., R.L.M.); and Chromex, Inc., 2705 B Pan American, Albuquerque, New Mexico 87107 (J.Z.)

Four Raman spectrometer configurations were compared for obtaining spectra of surface monolayers, including a new design that employed a line rather than point focus. Each spectrometer used a 514.5 nm laser and charge-coupled device (CCD) detector, but they differed in collection efficiency and sampling optics. Previously defined figures of merit for Raman signal and signal-to-noise ratio (SNR) were determined for each spectrometer, to aid quantitative comparison. The figure of merit for SNR, F_{SNR}, is demonstrated to be useful for comparisons because it permits prediction of SNR for a given spectrometer, sample, and measurement conditions. A rigorous definition of F_{SNR} is based on power density and takes into account the laser damage threshold of the sample. A simpler but less rigorous definition is based on laser power at the sample rather than power density and may be more useful to users who rarely determine the laser spot size. A new spectrometer design employing line focusing and collection is presented, with *f*/2 optics and a 6 mm slit image at the CCD. A proprietary aberration correction prevents slit image curvature common to most spectrographs with low *f*/#, and permits full height binning of the CCD. The line-focused spectrometer yielded an SNR and F_{SNR} which are comparable to those for a point focus using the same collection optics and slightly lower than those for the most efficient spectrograph examined. However, the line focus permitted much lower power densities to be employed, or yielded much larger signal for the same power density at a point focus. In quantitative terms, the new line-focused design yielded an SNR which is 67 times that of the best point-focused system, for the same sample, measurement time, and laser power density.

Index Headings: **Raman; Surface; Line focus; Raman figure of merit.**

INTRODUCTION

Through several advances in technique and instrumentation, surface Raman spectroscopy has developed to the point where it is possible to acquire spectra with an adequate signal-to-noise ratio from monolayers on various surfaces, including those that do not exhibit electromagnetic field enhancement.[1–4] This paper considers the case of a modern imaging spectrograph coupled to a charge-coupled device (CCD) detector operating in a range of 500 to 1000 nm. Once the instrument and geometry are optimized, the signal-to-noise ratio (SNR) is generally limited by three factors. First, the cross section number density product of the sample on the surface of interest determines the magnitude of the signal. Second, the noise level from sample or detector background contributes to the SNR, but can be mitigated by multichannel detection and extended observation time. Third, the signal and SNR may be increased by increasing the laser power density, up to the limit of sample radiation damage. For a given spectrometer and sample, the laser power density is generally increased to the threshold of sample damage.

An issue closely related to the ability to observe surface monolayers with Raman spectroscopy deals with comparisons of spectrometer designs. Since there are a number of variables that determine the SNR of a given experiment, direct comparisons are often difficult.[5] For example, the tighter laser focus of a Raman microscope may yield an SNR comparable to that of a less tightly focused but more efficient spectrometer, even for the same total laser power.[6] In addition, variations in integration time and the sample itself often frustrate comparisons of spectrometers intended for surface Raman. The figure of merit of the Raman signal, F_S, was defined previously in order to compensate for several experimental variables, as shown in Eq. 1.[5,7,8] F_S normalizes the observed signal for power density, sample cross section, number density, and integration time to yield a number that reflects several spectrometer variables. When comparing spectrometers, F_S provides a direct estimate of signal magnitude for the same power density, sample, and integration time. The related figure of merit for SNR was also defined,[5,8] as shown in Eq. 2. This value is more relevant to the success of the experiment because it incorporates the noise level and is directly related to the limit of detection. One objective of this paper is establishment of F_{SNR} as a useful means to evaluate spectrometer performance.

As noted earlier, surface Raman experiments are often limited by the radiation density tolerated by the sample. For a weakly adsorbed monolayer on an optically absorbing surface, the tolerance for laser power might be quite low,[2,3] in the region of 10–50 mW for a 50 μm diameter laser focus. One means to mitigate this problem is to increase the sample area monitored by the spectrometer. The use of a line focus has a precedent in Raman spectroscopy[2] and has the obvious advantage of distributing the laser power over a much larger area, thus lowering the power density for a given laser power. A line focus presents a problem, however, since efficient collection from a line becomes more difficult as the spectrometer becomes more efficient. A spectrometer with high collection efficiency and low *f*/# is subject to optical aberrations that create a curved image of the input slit at the detector. The second objective of the work presented here is demonstration of an efficient *f*/2 imaging spectrograph that collects light from a 6 mm line focus. The performance of the spectrograph was evaluated with several monolayer samples on glassy carbon surfaces by determining F_{SNR}. Finally, the new spectrometer is com-

Received 11 December 2000; accepted 26 February 2001.
* Author to whom correspondence should be sent.

0003-7028/01/5506-0767$2.00/0

TABLE I. Spectrometer configurations.

Number	Collection lens	Spectrograph	Ω^a_D, (sr)	A^a_D, (cm^2)	Detector[b]
1	Canon 50 mm, f/1.4	Kaiser 1.8i, 85 mm	0.35[c]	2×10^{-5}	TK512 BI 512 × 512[d]
2	Nikkor 50 mm, f/1.8	Chromex f/2, 135 mm	0.20	1.5×10^{-3}	Andor BI[d] 1024 × 256
3	Olympus 100× objective	Dilor f/6, 600 mm	[e]	3.1×10^{-8}	ISA FI 2000 × 800
4	Minolta 50 mm, f/1.7	Dilor f/6, 600 mm	[e]	2.0×10^{-5}	ISA FI 2000 × 800

[a] Estimated value, at the sample.
[b] BI = back illuminated. FI = front illuminated.
[c] Assumes f/1.5 collection, limited by spectrograph.
[d] Horizontal × vertical pixel format.
[e] Not determined, due to uncertainty about which of several apertures between slit and sample determine Ω.

pared to previous designs by using the figure of merit as a quantitative indication of SNR.

THEORY

The initial definition of F_s and F_{SNR} are repeated in Eqs. 1 and 2.[5]

$$F_s = \frac{S_{obs}}{P_D \beta_A D_A t_M} = A_D \Omega T Q K \quad \text{and} \tag{1}$$

$$F_{SNR} = \frac{SNR_{obs}}{(P_D \beta_A D_A t_M)^{1/2}} = (A_D \Omega T Q K)^{1/2} \tag{2}$$

where S_{obs} is the observed signal for a particular Raman band, in electrons; SNR_{obs} is the observed SNR for a particular Raman band; β_A is the differential Raman cross section (cm^2 molecular^{-1} sr^{-1}); D_A is the sample number density (molecule cm^{-3}); t_M is the total measurement time; A_D is the area of sample monitored (cm^2); P_D is the power density (photons cm^{-2} s^{-1}), assumed to be constant over the area A_D and through the sample; Ω is the collection solid angle at sample (sr); T is the spectrometer transmission (unitless); Q is the detector quantum efficiency (e^{-1} photon^{-1}); and K is the geometric factor that depends on sampling configuration (usually in cm).

The right sides of Eqs. 1 and 2 are based on certain assumptions about the sampling geometry, such as the relation between laser focal diameter and A_D. Nevertheless, the definition of F_{SNR} as the ratio of the observed SNR to $(P_D \beta_A D_A t_M)^{1/2}$ provides a useful indication of the anticipated SNR for a given sample, integration time, and power density. Stated differently, F_{SNR} adjusts the observed SNR for variations in sample dependent parameters, P_D, and t_M, and provides an indication of spectrometer performance for a range of samples, laser powers, and measurement times. In principle, the SNR for any sample, P_D and t_m may be predicted from F_{SNR}. For the case of surface monolayers, laser damage usually determines an upper limit for P_D, so one can predict the acquisition time required to achieve a given SNR for a monolayer with known β_A and D_A.

For a surface scatterer, it is more convenient to define D_S as molecules cm^{-2}, and K equals 1.[1,5] For this case, the units of F_{SNR} are cm sr$^{1/2}$ photon$^{-1/2}$. Defined in this manner, F_{SNR} is directly related to power density and incorporates possible limitations due to sample damage. However, power density is not commonly determined, and it is much more common to consider total laser power at the sample, in watts or photons s^{-1}. With the use of P_0 to denote total laser power in watts, and A_L to denote the area illuminated by the laser, an alternative figure of merit results:

$$F'_{SNR} = \frac{SNR_{obs}}{(P_o \beta_A D_S t_M)^{1/2}} = \left(\frac{A_D}{A_L} \Omega T Q\right)^{1/2} \tag{3}$$

F'_{SNR}, with units of sr$^{1/2}$ W$^{-1/2}$ s$^{-1/2}$, avoids the need to determine A_L and uses a more common unit for laser power. F'_{SNR} is less informative than F_{SNR} for samples that are subject to damage by high power density. Stated simply, F'_{SNR} provides a comparison of SNR for different instruments for a given laser power, while F_{SNR} provides a similar comparison for a given laser power density. Since the laser power density is not constant across A_L, both F_{SNR} and F'_{SNR} provide approximate rather than exact comparisons of relative SNR for different spectrometer designs. Furthermore, there are important differences in the applicability of F_{SNR} or F'_{SNR}, as will be discussed later.

EXPERIMENTAL

The spectrometer configurations employed are summarized in Table I. Spectrometers #1, #3, and #4 utilized 180° backscattered geometry and a 514.5 nm laser, and all laser powers cited were determined at the sample position. Spectrometer #1 has been described previously,[9] and spectrometers #3 and #4 are based on a commercial Dilor x-y imaging Raman spectrometer operating as a single spectrograph (600 mm, 1800 lines/mm grating, with holographic notch filter). Spectrometer #3 used an Olympus BX 40 microscope with a 100× objective and broadband beamsplitter, while #4 used ''macro'' sampling with a 50 mm camera lens. The Kaiser 1.8i spectrometer (#1) was purchased with f/1.4 lenses, to decrease the effective aperture ratio to f/1.5. Table I lists the A_D and Ω_D determined or estimated at the sample, as well as the CCD detector type. A_D is the smaller of the laser focal area or the slit image, at the sample.

Spectrometer #2 used a 514.5 nm laser incident on the sample at 45°, with collection at 0° relative to the surface normal. A line focus was generated with a Powell lens (Lasiris, P-5°, Lasiris, Inc., Quebec) preceding a 50 mm focusing lens. The Powell lens creates a line with a relatively flat laser intensity profile,[10] observed with a diode array detector to be flat to ±10%. The line dimensions at the sample were approximately 25 μm × 6 mm, and the power density was assumed to be constant across this area. The Andor back-illuminated CCD (1024 × 256 pix-

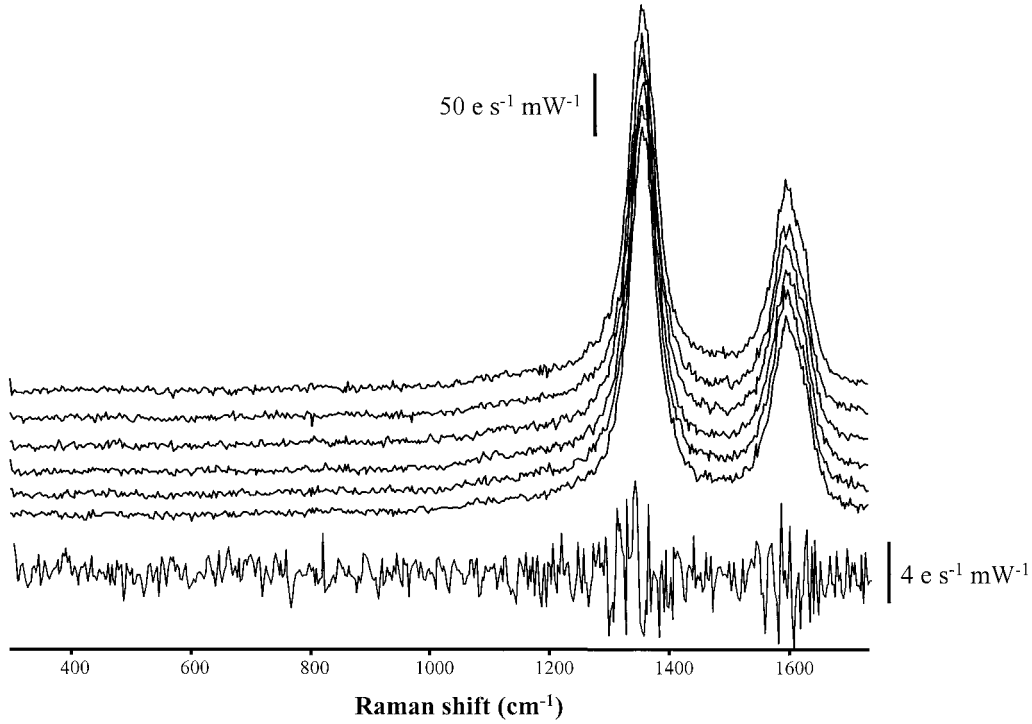

FIG. 1. Six repetitive spectra of GC20 obtained with spectrometer #1, with 10 mW of 514.5 nm laser power at the sample, 1 s integration time. Lower trace is the difference of two successive spectra.

els) detector was thermoelectrically cooled to −85°C, with the use of 10°C circulating water as a heat sink.

The spectrograph in configuration #2 was a custom design from Chromex, Inc. (Albuquerque, NM). The spectrograph accepts collimated light, and focuses it with a 50 mm *f*/1.8 Nikon camera lens onto a fiber array input coupler. The height of the fiber array is matched to the CCD and is about 6.7 mm. The light then exits the fiber array and is collimated by a 135 mm *f*/2 Nikon camera lens, dispersed by a 2000 groove/mm holographic reflectance grating, and then focused by another 135 mm *f*/2 Nikon camera lens onto the CCD camera. Normally, a dispersive spectrograph with a straight entrance slit yields curved spectral images of the slit on the focal plane, thus degrading spectral resolution when a CCD detector is used and the curved image is binned. Spectrograph #2 uses a proprietary curvature correction design to yield straight images on the CCD, which allows binning the entire CCD height without loss of spectral resolution. All spectra reported for spectrometer #2 used full height binning of all 256 pixels before digitization during readout.

Laser power was measured at the sample location with a Coherent "Field Master" power meter with an LM-2 power head and 1000:1 attenuator. For the line focus at powers above 50 mW, an LM-3 head was used. The figures of merit are stated in units of $sr^{1/2}\ W^{-1/2}\ s^{-1/2}$ (for F_{SNR}) or $e^-\ sr\ W^{-1}\ s^{-1}$ (for F'_S). The more fundamental but less convenient F_{SNR} is stated in units of $cm\ sr^{1/2}\ photon^{-1/2}$. Values based on peak height or peak area are so indicated in the text and tables.

All spectra were analyzed with Grams software (Version 4.02 from Galactic Industries, Salem, NH). Peak integration was carried out with the Grams "integrate" function (integrate.ab) with subtraction of a linear baseline drawn between 1150 and 1480 cm^{-1}.

RESULTS AND DISCUSSION

The first issue tested was the invariance of F_{SNR} with integration time and laser power. For glassy carbon (GC) as the sample, the region probed by Raman is an ~200 Å thick layer of the GC surface. The quantity $\beta_A D_S$ in Eq. 2 is $1.3 \times 10^{-10}\ sr^{-1}$,[3] with the easily validated assumption that the sampling depth (~ 200 Å) is thin compared to the spectrometer depth of focus (~100 μm). For the case of GC, $\beta_A D_S$ includes a factor which accounts for the attenuation of both laser and scattered light within the sample.[3] Equation 2 predicts how the observed SNR for the GC 1360 cm^{-1} band observed with a 514.5 nm laser varies as a function of integration time and laser power. The SNR for a given power and time was determined by acquiring six successive spectra under identical conditions, then calculating the SNR as the ratio of the mean area of the 1360 band (determined with the Grams "integrate" function as the peak area between 1150 and 1480 cm^{-1}, above a linear baseline) divided by the standard deviation of the six peak area determinations. Figure 1 shows a typical data set of six spectra for the determination of SNR. The difference of two spectra is also shown, demonstrating the increase in shot noise at the peak maxima.

Table II lists the results of F'_{SNR} determinations for a range of laser powers and integration times. For fixed integration time and varying laser power (line 1), six determinations of F'_{SNR} (comprising 36 spectra) yielded a mean F'_{SNR} of $5.71 \times 10^7\ (sr/W\ s)^{1/2}$ and a relative standard deviation (RSD) of 14%. F'_{SNR} determined for several laser powers and integration times (lines 2–4) yielded similar values, with an overall average of 24 determinations of $5.19 \times 10^7\ (sr/W\ s)^{1/2}$. F'_{SNR} shows no trends with power or integration time for a given spectrometer,

TABLE II. Figures of merit for GC 1360 cm^{-1} band (1150–1480 cm^{-1})[a].

	Spectrometer	F'_{SNR} (area)[b]	F'_{SNR} (height)[b]	F'_S (area)[c]
1.	#1, 1 s, 5–50 mW	5.71×10^7 (14%)[e]	7.72×10^7 (33%)[d]	1.47×10^{17} (28%)[e]
2.	#1, 20 mW, 1–10 s	5.03×10^7 (11%)	8.36×10^7 (46%)	1.42×10^{17} (1.3%)
3.	#1, 30 mW, 1–10 s	4.84×10^7 (6%)	1.27×10^8 (64%)	1.51×10^{17} (1.7%)
4.	#1, 40 mW, 0.5–10 s	5.19×10^7 (15%)	8.04×10^7 (31%)	1.44×10^{17} (2.4%)
5.	#1 mean	5.19×10^7	9.21×10^7	1.46×10^{17}
6.	#2 line 31.5 mW, 1–10 s	4.02×10^7 (63%)	3.28×10^7 (16%)	3.91×10^{16} (21%)
7.	#3, 100× micro 11.7 mW, 1–120 s	5.24×10^6 (13%)	1.27×10^7 (18%)	2.52×10^{15} (12%)
8.	#4, macro, f/2 73 mW, 10–30 s	3.39×10^6 (52%)	4.01×10^6 (57%)	3.07×10^{14} (0.3%)

[a] Integration range for 1360 cm^{-1} Raman band.
[b] Units are sr$^{1/2}$ W$^{-1/2}$ s$^{1/2}$.
[c] Units are e$^-$ cm sr W^{-1} s^{-1}.
[d] Relative standard deviation for six determinations of F'_{SNR} or F_{SNR}, each at a different power. Each determination consisted of six spectra, in order to evaluate the SNR.
[e] RSD of determinations of peak area for six successive spectra.

indicating that Eq. 2 is valid for the conditions employed. Since A_D, A_L, Ω, T, and Q are constant for a given spectrometer, the SNR shows the expected dependence on power and time stated in Eq. 2.

A figure of merit for signal, rather than SNR, has also been defined[5,8] as in Eq. 4 for the case of a surface scatterer:

$$F'_S = \frac{S_{obs}}{(P_o \beta_A D_S t_M)} = \left(\frac{A_D}{A_L}\Omega T Q\right) \quad (4)$$

F'_S is proportional to the signal from the spectrometer, normalized for laser power, cross section, number density, and measurement time; hence it indicates a spectrometer sensitivity. F'_S is also listed in Table II for GC on the Kaiser spectrometer and a variety of integration times and laser powers. The invariance of F'_S indicates that Eq. 4 applies, with no significant signal contributions from dark current, offset, etc. The mean value of 24 determinations of F'_S on the Kaiser system was 1.46×10^{17} e$^-$ sr W^{-1} s^{-1}. F'_{SNR} and F'_S were determined less extensively for three other spectrometer configurations by considering a single laser power and three integration times. As before, each determination involved six successive spectra to determine the mean and SNR of the peak area. The results are listed in lines 6–8 of Table II. F'_{SNR} and F'_S are restated in Table III, normalized to the average Kaiser values.

The relative magnitudes of F'_S and F'_{SNR} listed in Tables I and II are reasonable in light of Eqs. 3 and 4. The Kaiser spectrometer has the highest Ω and T of systems tested. Since Ω is proportional to $(f/\#)^{-2}$, the $f/1.5$ Kaiser is expected to have a higher F'_S than the Chromex system ($f/2$) by a factor of 1.8 from the Ω factor and another 50% from higher T due to losses in the Chromex fiber array. The Dilor system is $f/6$ and has more mirrors and steering optics—hence lower Ω and T. Equations 3 and 4 predict that F'_{SNR} should track $(F'_S)^{1/2}$, and this relationship is observed experimentally. The observed range in F'_S is a factor of 475, while that of F'_{SNR} is a factor of 14. Stated differently, spectrometer #1 will yield an SNR that is 14 times higher than spectrometer #4 for the same laser power, integration time, and sample.

TABLE III. Figures of merit, based on GC 1360 cm^{-1} peak area.

	Spectrometer	F^a_{SNR}	F_{SNR} (relative)[b]	F'_{SNR} (relative)[b]	F'_S (relative)[b]
1.	#1 50 μm spot	1.45×10^{-4}	1.00	1.00	1.00
2.	#2 line focus	9.80×10^{-3}	67	0.77	0.26
3.	#3, micro 100×	5.69×10^{-7}	0.0039	0.10	0.020
4.	#4 macro	9.49×10^{-6}	0.065	0.07	0.0021

[a] Determined by multiplying F'_{SNR} by $A_L^{1/2}$ [units are cm$^{3/2}$ sr$^{1/2}$ (photon)$^{-1/2}$].
[b] Normalized to the corresponding figure of merit for spectrometer #1.

When examining surfaces, F'_{SNR} as listed in Tables II and III can be quite misleading. When the laser intensity is limited by sample damage, it is power density rather than power that determines the limit. For example, spectrometers #3 and #4 yield approximately the same SNR for a given laser power at the sample, but spectrometer #3 has over 600 times the power density. F_{SNR} as defined in Eq. 1 is based on power density rather than power and permits a more useful comparison when laser damage is an issue. F_{SNR} is proportional to the observed SNR for a given power density, measurement time, and sample. It may be calculated by multiplying F_{SNR} by $A_L^{1/2}$, under the assumption of uniform power density over the area illuminated by the laser. A more subtle assumption is the invariance of the power density causing sample damage with illumination geometry. As noted recently by Zhang et al.,[12] the damage threshold may vary with the illumination area due to more efficient heat conduction away from small illumination areas. This effect partially mitigates possible sample damage for a tight laser focus for the case of a thermal mechanism and a conductive sample. Since the effect depends on the damage mechanism, sample properties, and illumination geometry, it is not included in the calculation of F'_{SNR}, and the threshold power density for sample damage is assumed to be constant for a given sample, regardless of illumination geometry. F_{SNR} values for all four spectrometers determined under these assumptions and based on the GC 1360 cm^{-1} band area are listed in Table III.

A clear difference between F_{SNR} and F'_{SNR} arises when considering spectrometers #1 and #2. The $f/2$ system (#2) has a smaller F'_S due to its lower Ω, and a similar but smaller difference is apparent in F'_{SNR} for the two configurations. For a given laser power and sample, spectrometer #2 yields a slightly lower SNR than #1. However, for a given power *density,* spectrometer #2 yields a much higher SNR, by a factor of 67. If the power density were increased to a point just below the sample damage

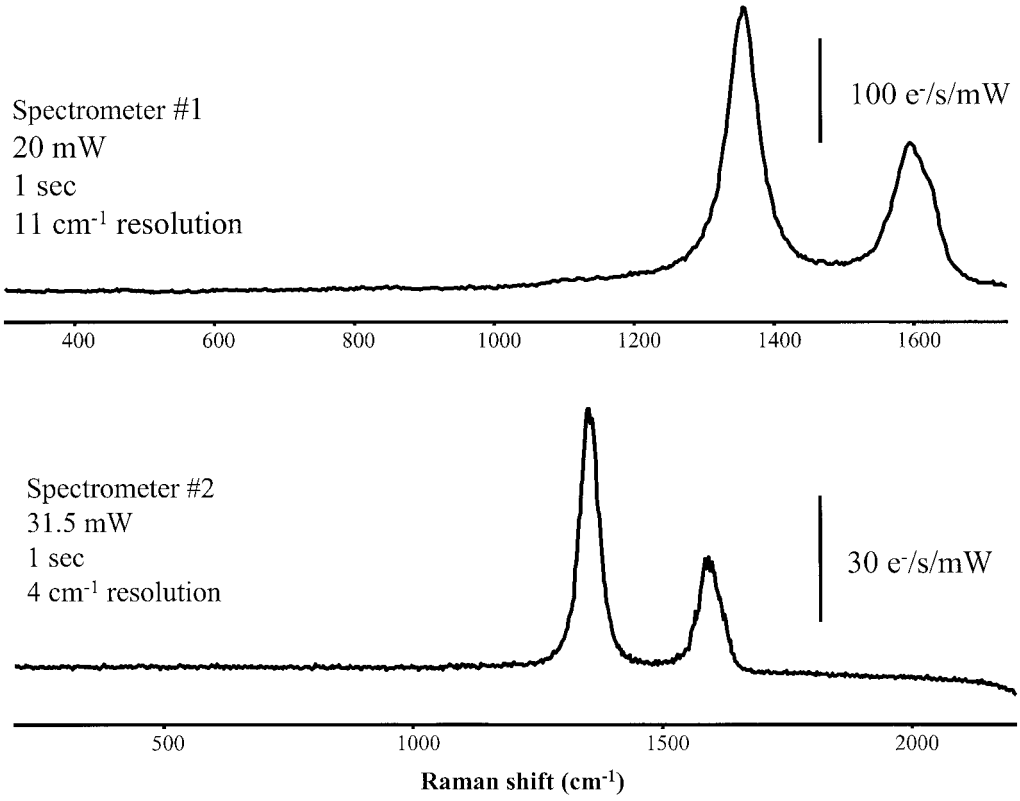

FIG. 2. Spectra obtained with spectrometers #1 and #2, with conditions as shown. The larger format of the CCD detector covers a wider spectral range for spectrometer #2.

threshold for both spectrometers #1 and #2, the F_{SNR} predicts that the SNR for spectrometer #2 will be 67 times that of #1. For example, the power density for the spectra of Fig. 5 was 180 w/cm^2, while for Fig. 2 (top) it was 1000 w/cm^2, but the SNR and resolution in Fig. 5 were higher than those in Fig. 2.

GC spectra obtained with spectrometers #1 and #2 are compared in Fig. 2. As predicted from F'_S, #1 is more

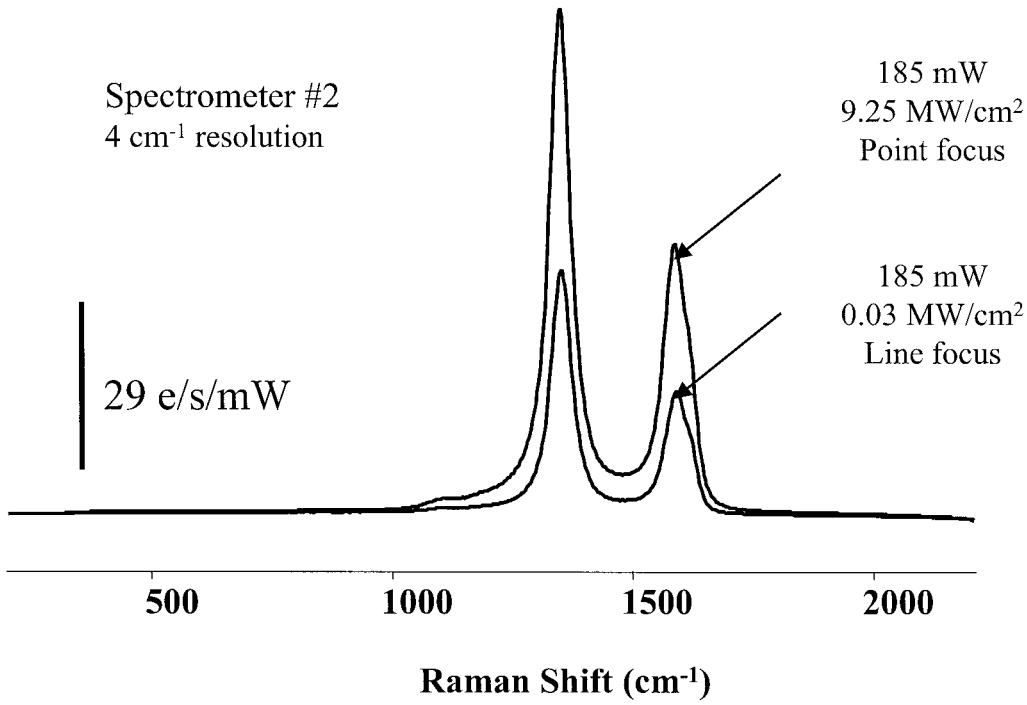

FIG. 3. Comparison of point and line focus for spectrometer #2, with the same total power at the GC sample. Intensity scale is the same for both spectra, as was the integration time (1 s).

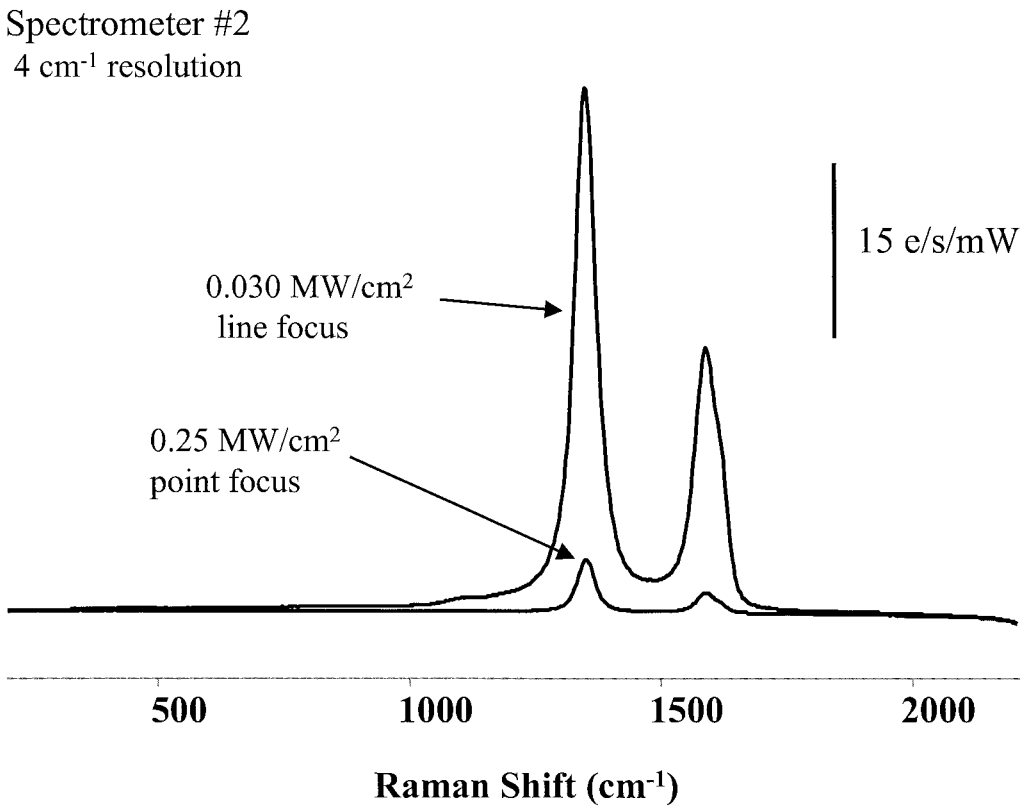

FIG. 4. GC spectra from spectrometer #2, for point and line focus, with the power densities indicated. Integration time = 1 s in both cases.

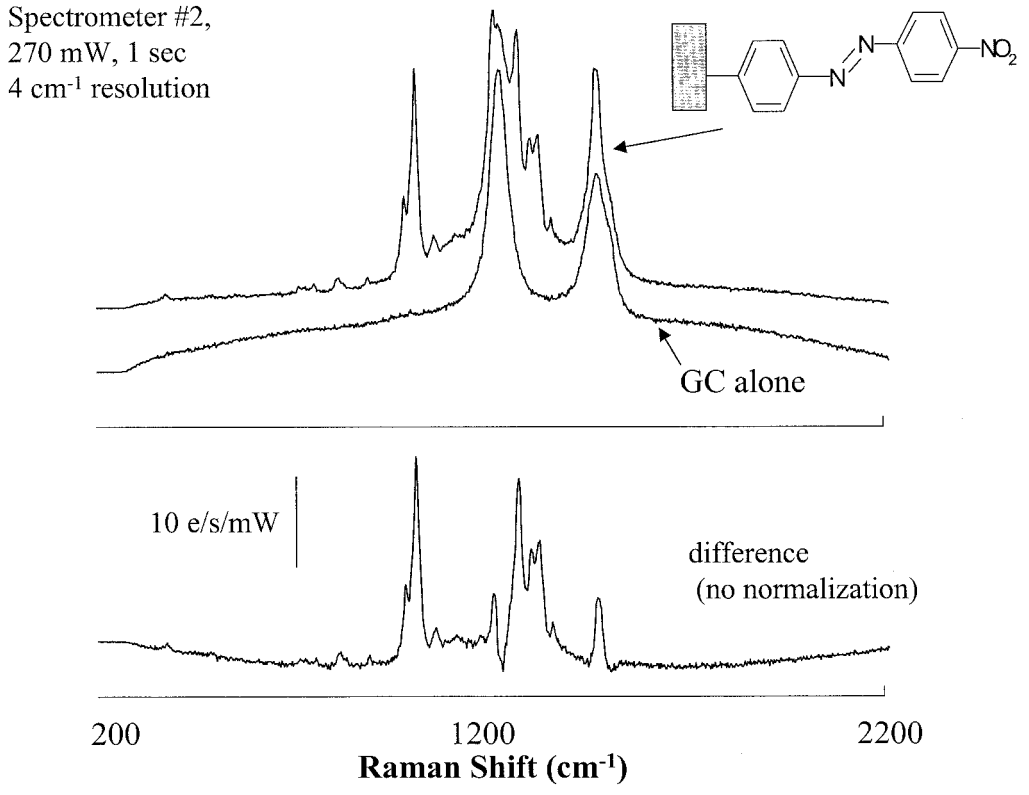

FIG. 5. Spectra of unmodified GC and of a chemisorbed monolayer of nitroazobenzene on GC obtained with spectrometer #2. Sample prepared as described in Ref. 9.

sensitive than #2 for a given laser power. Spectrometer #2 has a larger detector and, hence, greater wavelength coverage and resolution. Figure 3 illustrates the advantage of a line focus compared to a point focus on the same spectrometer #2. The peak area is slightly smaller for the line at a given laser power, because the 6 mm line is not collected as efficiently at the point focus, by about 50%. However, the small decrease in signal and SNR with the line focus is accompanied by a large decrease in power density, by a factor of 300 in this case. Figure 4 reiterates this issue, illustrating that the line focus yields much higher signal and SNR even when the power density is a factor of 8 lower than that of the point focus. Figure 5 illustrates the use of the line focus of spectrometer #2 for obtaining a Raman spectrum of a chemisorbed monolayer of nitroazobenzene.[9] The relatively high laser power of 270 mW produces a power density that is much lower than the point focus used in spectrometer #1, yet the SNR, resolution, and signal magnitude were all better for the line focus.

The spectrometer designs considered here may be compared to those reported previously[3,9,11] by calculating a figure of merit from published spectra. The signal in terms of $e^- s^{-1} W^{-1}$ for the peak height may be converted to F'_s by dividing the peak height by $\beta_A D_S$ (1.3×10^{-10} sr^{-1}). For example, the F'_s for a Chromex $f/4$ spectrometer determined from a GC sample[3] is 8×10^{14} $e^- sr\ W^{-1}$ s^{-1}, compared to spectrometer #1, with a value of 2.4×10^{15}. Similarly, F'_s for the Kaiser 1.8i with different collection optics[9] is 3×10^{14}. It should be noted that these comparisons used the same laser wavelength (514.5 nm) and sample (GC) but varying laser power densities. Peak areas were not available for the older experiments, preventing direct comparison with the last column of Table II.

CONCLUSION

Figures of merit based on power density (F_{SNR}) and total laser power (F'_{SNR}) provide a means to compare spectrometer performance for surface Raman spectroscopy. If the figure of merit for a given spectrometer is known, the expected SNR may be determined readily from laser and sample parameters. F_{SNR} is more general and more rigorous than F'_{SNR} because it accounts for laser power density. Since sample damage by the laser is often a limiting factor in surface Raman spectroscopy, F_{SNR} permits prediction of SNR at power densities below a level where sample damage occurs. F'_{SNR} is simpler to use because it does not require knowledge of the laser focal area. However, a high F'_{SNR} does not necessarily indicate a higher SNR for a surface Raman experiment, since the laser may be focused sufficiently tightly to cause sample damage. This issue is mitigated by the use of a line focus and imaging spectrometer, which permit much higher total laser power while maintaining relatively low laser power density. The result is higher SNR below the sample damage threshold. Of course, the damage threshold is strongly dependent on the nature of the sample, the illumination geometry,[12] and the damage mechanism. Nevertheless, a spectrograph capable of monitoring a larger sample area will yield higher SNR for a given power density below the damage threshold. Stated differently, a line focus permits a higher laser power to be used before the sample damage threshold is reached.

1. R. L. McCreery, *Raman Spectroscopy for Chemical Analysis,* Wiley Chemical Analysis Series, Vol. 157, J. Winefordner, Ed. (John Wiley, New York, 2000), Chap. 13.
2. W. B. Lacy, J. M. Williams, L. A. Wenzler, T. P. Beebe, and J. M. Harris, Anal. Chem. **68,** 1003 (1996).
3. M. R. Kagan and R. L. McCreery, Langmuir **11,** 4041 (1995).
4. V. M. Hallmark and A. Campion, J. Chem. Phys. **84,** 2933 (1986).
5. M. Fryling, C. J. Frank, and R. L. McCreery, Appl. Spectrosc. **47,** 1965 (1993).
6. R. L. McCreery, *Raman Spectroscopy for Chemical Analysis,* Wiley Chemical Analysis Series, Vol. 157, J. Winefordner, Ed. (John Wiley, New York, 2000), Chap. 11.
7. K. G. Ray and R. L. McCreery, Appl. Spectrosc. **51,** 108 (1997).
8. R. L. McCreery, *Raman Spectroscopy for Chemical Analysis,* Wiley Chemical Analysis Series, Vol. 157, J. Winefordner, Ed. (John Wiley, New York, 2000), Chap. 13, pp. 45–47, p. 65.
9. Y.-C. Liu and R. L. McCreery, Anal. Chem. **69,** 2091 (1997).
10. K. Christensen and M. Morris, Appl. Spectrosc. **52,** 1145 (1998).
11. M. A. Fryling, J. Zhao, and R. L. McCreery, Anal. Chem. **67,** 967 (1995).
12. D. Zhang, J. D. Hanna, Y. Jiang, and D. Ben-Amotz, Appl. Spectrosc. **55,** 61 (2001).